

RSC Advances



This is an *Accepted Manuscript*, which has been through the Royal Society of Chemistry peer review process and has been accepted for publication.

Accepted Manuscripts are published online shortly after acceptance, before technical editing, formatting and proof reading. Using this free service, authors can make their results available to the community, in citable form, before we publish the edited article. This *Accepted Manuscript* will be replaced by the edited, formatted and paginated article as soon as this is available.

You can find more information about *Accepted Manuscripts* in the [Information for Authors](#).

Please note that technical editing may introduce minor changes to the text and/or graphics, which may alter content. The journal's standard [Terms & Conditions](#) and the [Ethical guidelines](#) still apply. In no event shall the Royal Society of Chemistry be held responsible for any errors or omissions in this *Accepted Manuscript* or any consequences arising from the use of any information it contains.

24 1. Introduction

25 Gelatin is a peptide molecule polymeric material, obtained from a hydrolytic
26 treatment of collagen under acidic or alkaline conditions. The triple helix structure of
27 collagen partially separates, ruptures and non-uniform mixture of polypeptides with
28 different amino acid are formed [1]. Because of its good biological properties and low
29 toxicity, gelatin is widely used as different kinds of materials, such as sponges, films,
30 microballoon, scaffolds, nanoparticles and bandages etc [2-6]. However, the relatively
31 weak thermal stability, poor mechanical properties and easily-degradable quality limit
32 the potential application of gelatin as a practical material [7]. Microcrystalline
33 cellulose (MCC), a linear polysaccharide combining of β -glucoside keys, is usually
34 blended with gelatin to overcome obstacles of the biopolymer matrix [8-10]. Its
35 excellent properties, such as renewable origin, biodegradable-ability of their
36 components, environmental-friendly and non-toxic character further broaden its
37 usages [10-13]. Ethylenediamine tetraacetic dianhydride (EDTAD) is used as
38 chelating reagent in common studies [14]. Its biodegradable behavior and special
39 molecular structure, which consists of two anhydride groups that can react with
40 hydroxyl or amine groups, ensure its function in modification of biomaterials [15-16].

41 Recent years, a great number of researchers worldwide have been devoting to
42 modification of gelatin with various crude macromolecules, such as cellulose,
43 chitosan, starch, montmorillonite, polyvinyl alcohol, zeolite etc [17-22]. Jridi et al. [23]
44 investigated the physical, structural, antioxidant and antimicrobial properties of
45 gelatin/chitosan composite films and chose the best proportion of the two components
46 to be applied as food package material; Li et al. [24] prepared an active gelatin-based
47 films incorporated with five kinds of natural antioxidants and compared the function
48 of these extracts on the antioxidant, physical and mechanical properties of the films;
49 Alves et al. [25] studied the effect of three components (gelatin, cellulose, starch) on
50 the biodegradation, water vapor permeability and mechanical properties of the starch/
51 cellulose/gelatin nanocrystals films by orthogonal experiments; Andrade et al. [26]
52 reported a new edible coating materials containing gelatin and cellulose nanofibers,
53 and evaluated the watability of the coating film on banana and eggplant epicarps.

54 Unfortunately, the existing modification way of gelatin-based composite films with
55 natural polymers, especially cellulose, are mostly prepared by blending method, in
56 which the hydrogen bond or electrostatic interactions is used to explain the
57 mechanism of the polymer matrix. Not exact chemical reaction happened between
58 gelatin and original cellulose. Therefore, proper chemical modification on cellulose is
59 needed to make the crosslinking reaction with gelatin possible. Cheng et al. [27]
60 oxidized cellulose by periodate oxidation to obtain 2, 3-dialdehyde cellulose (DARC),
61 which then reacted with collagen via the Schiff base reaction between -NH_2 in
62 collagen and -CHO in DARC backbone to obtain DARC/Col composite films; Li et al.
63 [28] employed the same oxidation process to oxidize carboxymethyl cellulose and the
64 product with two aldehyde groups reacted with gelatin to prepare edible film material.

65 Lately, a novel crosslinker N-hydroxysuccinimide (NHS) active ester, which is
66 synthesized by reaction between carboxylic acid and NHS in the presence of
67 carbodiimide [29], attracted extensive attention mainly due to their cytocompatibility,
68 biocompatibility and availability [30-31]. Furthermore, Gil's group [32] concentrated
69 on modifying sugarcane bagasse, which was the raw material of cellulose, with
70 EDTAD to gain the ester group that used as an absorbent material. In light of these
71 researches, the hydroxyl and/or carboxyl function groups in these three biological
72 polymers (gelatin, cellulose and EDTAD) further guaranteed the chemical reaction to
73 produce materials with new properties [33].

74 In this paper, microcrystalline cellulose was modified with EDTAD to get a new
75 type of cellulose ester MCC-EDTAD (ME). And then, a novel macromolecule
76 crosslinker N-hydroxysuccinimide activated MCC-EDTAD ester (MCC-EDTAD-
77 NHS, MEN) was firstly synthesized in the presence of 1-(3-dimethylaminopropyl)-3-
78 ethyl-carbodiimide hydrochloride (EDC) to react with gelatin (Scheme 1), and the
79 biological polymer film with new qualities was recorded. Testing instruments, such as
80 FTIR, XRD, TGA-DSC, mechanical property, contact angles and residual amino
81 group test were applied in our present study. Additionally, in vitro degradation studies,
82 light barrier properties and water uptake measurement of crosslinked gelatin films
83 were investigated. On the basis of these results, the comparison of thermal stability

84 and light barrier properties between MEN modified gelatin films (Gel-MEN) and
85 cellulose blending films (Gel/MCC) were explored.

86 Scheme 1 here

87 **2. Experimental**

88 **2.1 Materials**

89 Gelatin (type A, obtained from pigskin, with an approximate molecular weight of
90 50,000 and isoelectric point at pH=8 determined by fluorescence measurements) was
91 obtained from Sinopharm Chemical Reagent Co., Ltd. MCC (extra pure, average
92 particle size 90 μm), NHS (AR, 98%) and EDC (AR, 99%) were purchased from
93 Energy Chemical Technology Co., Ltd (Shanghai). Glycerol (AR, 99%), DMF (AR,
94 99.5%), EDTA disodium salt (AR, 99%), acetic anhydride (AR, 98.5%) and other
95 agents were obtained from Tianjin Fu Yu Fine Chemical Co., Ltd. All chemicals and
96 reagents were used as received without further purification.

97 **2.2 Preparation of MEN**

98 2.2.1 Synthesis of EDTA dianhydride (EDTAD)

99 The EDTA dianhydride was prepared using the method described by Gil [34] with
100 EDTA disodium salt and acetic anhydride as ingredients. 25 g EDTA disodium was
101 dissolved in 250 ml distilled water to get the clear solution, and then HCl was added
102 dropwise until precipitation of EDTA occurred. The precipitate was vacuum filtered
103 and rinsed with 99% EtOH, 99% diethyl ether, subsequently dried in an oven at 70 $^{\circ}\text{C}$
104 and cooled in a desiccator prior to use.

105 For the preparation of EDTA dianhydride, 18 g EDTA was suspended in 50 ml
106 pyridine and 25 ml acetic anhydride was added. Then the mixture was heated under
107 reflux and kept stirring at 65 $^{\circ}\text{C}$ for 24 h. After reaction, the solid obtained was
108 vacuum filtered, rinsed in diethyl ether and dried under vacuum at 50 $^{\circ}\text{C}$. The
109 prepared EDTAD was characterized by $^1\text{H-NMR}$ spectrum (Bruker Advance 400
110 spectrometer) and FTIR spectrum (Nicolet NEXUS 470 FT-IR spectrometer).

111 2.2.2 Synthesis of MCC-EDTAD (ME)

112 The functionalization of MCC with EDTAD was carried out according to Gil's
113 group [35] with slight modification. 9 g MCC and 3 g EDTAD were suspended in 100
114 ml DMF, and then the mixture was shaken and heated under reflux at 75 $^{\circ}\text{C}$ for 24 h.
115 The modified materials were elaborated by filtration under reduced pressure, washed
116 in a row with DMF, distilled water, saturated NaHCO_3 solution (in order to release

117 carboxylate and amine functions), distilled water, and then with ethanol. After dried
118 under vacuum at 50 °C, the mass percent gains were calculated by equation (1).

$$119 \quad \text{Weight gain(\%)} = \frac{m_{\text{modified}} - m_{\text{unmodified}}}{m_{\text{unmodified}}} \times 100 \quad (1)$$

120 2.2.3 Synthesis of NHS active MCC-EDTAD ester (MEN)

121 MEN was synthesized by the method of Li [36] with a bit improvement. Mixed
122 solution was prepared by dissolving 12.5 mmol ME, 50.0 mmol NHS, 50.0 mmol
123 EDC together in 200 ml distilled water and gently stirred at 40 °C for 1 h. After
124 reaction, the solid was vacuum filtered, and then washed with distilled water several
125 times, dried under vacuum at 50 °C to get purified MEN. The mass percent gains were
126 also calculated by equation (1). The ME and MEN obtained were characterized using
127 FTIR spectrum (Nicolet NEXUS 470 FT-IR spectrometer), Elemental Analyzer
128 (Vario EL III, Elementar Analysensysteme, Germany) and TGA-DSC (Q600SDT,
129 TA, USA).

130 2.3 Modification process and film formation

131 Gelatin solution (3%, w/v) was prepared by dissolving gelatin powder in distilled
132 water and then heated at 45 °C for 2 h under continuous stirring. Glycerol was added
133 as plasticizer at a certain concentration (15% of dry gelatin weight). The dosage of
134 MEN was determined by mass ratio with gelatin, which meant $m_{\text{MEN}}/m_{\text{gelatin}}=0\%$,
135 5%, 10%, 15%, 20%, 25%, 30%. So the corresponding modified gelatin samples were
136 named as Gel, Gel-5%MEN, Gel-10%MEN, Gel-15%MEN, Gel-20%MEN,
137 Gel-25%MEN and Gel-30%MEN, respectively. Various weight of MEN powder was
138 dissolved in distilled water under stirring for 12 h at room temperature to produce a
139 suspension liquid. Then the solution was added dropwise to gelatin liquids, and acetic
140 acid (3% of water volume) was dripped into the whole system to promote the start of
141 the interfacial reaction. These mixtures were gently stirred for 12 h at 45 °C.

142 To cast the films, 30 g gelatin reaction solution was transferred into a teflon dish
143 and placed at room temperature for 2 h, then put in oven at 40 °C until films dried.
144 The dried films were peeled off and stored in a desiccator with relative humidity
145 $\leq 20\%$. Besides, one part of gelatin reaction solution was freeze dried at -55 °C, 70 Pa
146 with vacuum freeze drier (FD-1A-50, Beijing, China) and the lyophilized powder was
147 characterized by FTIR spectrum (Nicolet NEXUS 470 FT-IR spectrometer).

148 2.4 XRD analysis

149 XRD analysis of samples were performed on an X-ray diffractometer
150 (D8-ADVANCER, Bruker AXE, Germany) with a thin film attachment using Cu-K α
151 radiation ($\lambda=0.1541$ nm) at a current of 40 mA and an accelerating voltage of 40 kV.
152 The patterns were recorded from 10° to 60°.

153 **2.5 Determination of residual amino group in gelatin**

154 The residual -NH₂ groups in modified gelatin solution was determined by the
155 improved Van Slyke method at 45 °C [37-38]. Sample solutions were mixed with
156 acetic acid, sodium nitrite and stirred for 45 min. The residual primary amine (mol/g)
157 was calculated according to the volume of N₂. All samples were tested in triplicate.

158 **2.6 In vitro degradation studies**

159 The degradation study of gelatin films was carried out in vitro by incubating in
160 phosphate buffer (pH 7.40) at 37 °C for different intervals (1, 3, 5, 7, 9, 12 and 24 h),
161 which was developed from method of Haroun [39]. The gelatin films were dried at 60
162 °C to constant weight prior to use and marked as m_0 . After different degradation time,
163 the samples were washed with distilled water after filtrated under vacuum and dried at
164 60 °C to constant weight (m_t). The degradable performance was examined by the
165 weight remaining from Equation (2).

$$166 \text{ Weight remaining(\%)} = \frac{m_t}{m_0} \times 100 \quad (2)$$

167 **2.7 Scanning electron microscopy (SEM) of gelatin films**

168 The microstructures of the prepared films were investigated by Quanta 200
169 environmental scanning electron microscope (SEM, FEI Company, Holland). Before
170 observation, the film surfaces were coated with Au using SEM coating device. More
171 than ten micrographs were taken from different zones of each surface film.

172 **2.8 Thermo gravimetric analysis**

173 The thermal stability of gelatin film was determined by thermogravimetric and
174 differential thermal scanning calorimetry synchronous apparatus (TGA-DSC,
175 Q600SDT, TA, USA). The gelatin film samples (approximately 2.5 mg) were
176 weighed accurately into aluminium pans and sealed. The endothermal curve of the
177 crushed film was recorded from 20 °C to 500 °C at a scanning rate of 10 °C/min under

178 nitrogen atmosphere. Additionally, the thermal stability of Gel/MCC blending films
179 was also studied as compared with Gel-MEN films.

180 **2.9 Mechanical testing**

181 Prior to investigating the mechanical properties, films were conditioned for 48 h at
182 20 °C and 50±5% RH condition. Tensile strength (T_s), elasticity modulus (E_m) and
183 elongation at break (E_{ab}) were determined as described by Benjakul [40] with a slight
184 modification, using the Microcomputer Controlled Electronic Tensile Testing
185 Machine (WDL-005, Jinan, China) equipped with tensile load cell of 300 N. Samples
186 with initial grip length of 25 mm were used for testing and the cross-head speed was
187 set at 10 mm/min. The thickness of each film was measured by Vernier Caliper (0.02
188 mm/150 mm, Shanghai, China).

189 **2.10 Contact angles measurement**

190 The water contact angles (CAs) of all films were measured by the Sessile drop
191 method using a DSA100 contact angle measuring system from Krüss. The gelatin
192 reaction solution was coated on the surface of glass sheet to obtain films with
193 thickness about 0.1 mm, and then stored in a desiccator with relative humidity $\leq 20\%$.

194 **2.11 Light barrier properties and transparency**

195 The ultraviolet and visible light barrier properties of the films (1 cm×2 cm) were
196 measured by an ultraviolet-visible spectrophotometer (UV-7504C, Shanghai, China)
197 at selected wavelengths from 200 to 800 nm following Fang's method [41]. The
198 transparency value of films was calculated by the Equation (3), where T was
199 transmission (%) at each wavelength and x was film thickness (mm). According to the
200 equation, high transparency values indicate good light barrier performance.

$$201 \text{ Transparency value} = -\log T/x \quad (3)$$

202 **2.12 Water uptake measurement**

203 The water uptake measurement of the films was determined in the light of Kavosi
204 [42] and Tang [43] with a little development. Rectangular specimens sized 15 mm×10
205 mm with a thickness of 0.1 mm were prepared. The samples were conditioned at 20
206 °C in a desiccator containing silica gel (RH 20%±5%) three days to constant weight
207 (W_i). Then, the film samples were transferred into desiccators at 100% relative
208 humidity (supersaturated salt solution of $\text{CuSO}_4 \cdot 5\text{H}_2\text{O}$) at 20 °C for eleven days to

209 absorb water until the weight reached to equilibrium. The weight of samples at the
210 adsorption time of t was noted as W_t . The amount of water adsorbed at different
211 intervals and equilibrium were calculated as Equation (4). All tests are the means of at
212 least three measurements.

$$213 \quad \text{Water Absorption (\%)} = \frac{W_t}{W_i} \times 100 \quad (4)$$

214 **3. Results and Discussion**

215 **3.1 Characterization of MEN**

216 3.1.1 Spectra of EDTAD

217 ^1H NMR (400 MHz, DMSO, Fig. S1): δ 3.691 (s, 8H), 2.657 (s, 4H), 3.080 (s,
218 DMSO), 2.496-2.488 (m, DMSO), which were in accordance with the characteristic
219 peaks of H in the ideal product. The FTIR spectrum (Fig. S2) further proved the
220 dianhydride structure with two groups of splitting peaks. The peaks in high frequency
221 region splitted at 1813, 1759 and 1689 cm^{-1} , gap of 60 cm^{-1} between adjacent peaks.
222 The low frequency groups splitted at 1139, 1074, and 991 cm^{-1} with the same interval.
223 Additionally, the bands at 1245 and 1400 cm^{-1} related to C-O and C-N stretch
224 respectively were also evidence of EDTAD structure.

225 3.1.2 Spectra of MCC, ME and MEN

226 The FTIR spectra (Fig. S3) fully depicted the functional groups of MCC, ME and
227 MEN. Compared with MCC, the appearance of strong bands at 1741 cm^{-1} in ME can
228 be attributed to axial deformation of the ester bond, and bands at 1633, 1406 cm^{-1} are
229 attributed to asymmetric and symmetric axial deformations of carboxylate. These
230 bands confirmed the successful functionalization of MCC with EDTAD via formation
231 of ester linkages. For MEN, absorption peaks at 1706, 1210 and 811 cm^{-1} represented
232 γ -dicarbonyl stretching vibration, C-N stretching and C-C vibration respectively.
233 Specially, the reinforce of ester carbonyl band at 1742 cm^{-1} and the weakening of
234 carboxy carbonyl band at 1600 cm^{-1} further proved the structure of the active ester.

235 3.1.3 Elemental analysis and thermal properties of MCC, ME and MEN

236 As can be seen in Table 1, there was a considerable increase in nitrogen content
237 with 1.92% after functionalization of MCC with EDTAD. Accompanied by the

238 significant weight gain of 72.50%, the modified material (ME) with EDTAD
239 incorporated was obtained. Similarly, the element N increased to 2.48% in MEN,
240 0.50% higher than that of ME, which meant the esterification reaction happened
241 between ME and NHS with a five-membered nitrogenous ring linked. Also, the
242 weight gain of 30.80% further proved the truth.

243 The initial decomposition temperature at 5% weight loss (T_i), the maximum weight
244 loss temperature (T_m), the glass transition temperature (T_g) and the char residue at 500
245 °C of MCC, ME and MEN are recorded in table 1 (Fig. S4). T_i of MCC and ME was
246 309.10 °C and 271.45 °C, respectively while MEN was 222.54 °C, which suggested a
247 reduction in thermal stability. It can be related to the reaction activity of the three
248 materials with $-NH_2$ in gelatin, which was in accordance with the results of residual
249 amino group below. To summarize, the difference of each item further certified the
250 introduction of EDTA and NHS into MCC, which agreed with FTIR and elemental
251 analysis.

252 Table 1 here

253 3.2 Confirmation of MEN crosslinking with gelatin

254 3.2.1 FTIR spectra analysis of MEN, gelatin and Gel-MEN film

255 FTIR spectra of the pristine gelatin (curve a), pristine MEN (curve b), and
256 Gel-25%MEN film (curve c) are compared in Fig. 1. In the case of pristine gelatin,
257 the C=O stretching vibration appearing at 1664 cm^{-1} demonstrated amide I band,
258 while the amide band II was indicated by N-H bending vibration observed at 1535
259 cm^{-1} . Besides, aliphatic C-H bending vibrations were observed at 1450 cm^{-1} and bands
260 at $1331, 1230\text{ cm}^{-1}$ declared the C-N bond stretching vibrations. Gel-MEN showed all
261 the characteristic peaks of gelatin and MEN, such as 1643 and 1546 cm^{-1} . This
262 indicated the successful reaction between gelatin and crosslinker MEN along with a
263 representative peak at 1741 cm^{-1} , which clearly indicated the amidation reaction
264 between $-NH_2$ in gelatin and active ester base in MEN.

265 Fig. 1 here

266 3.2.2 X-ray diffraction studies of MEN, gelatin and Gel-MEN film

267 In order to examine the effect of MEN on crystal structure and crystallinity of

268 gelatin, XRD patterns of freeze-dried gelatin films are investigated. Data on 25%
269 MEN formulation are presented as a representative example. As shown in Fig. 2,
270 curve (a) was the XRD pattern of MEN, which displayed the typical XRD pattern of
271 the native cellulose with the main diffraction signals at around 14.9°, 16.2°, 22.5° and
272 34.3° [44]. The curve (b) only showed an extensive broadening peak in the 2 θ range of
273 15-25°, which was a typical XRD pattern of pure gelatin originated from α -helix and
274 triplehelical structure [45-46]. The XRD pattern of Gel-25%MEN film is given in Fig.
275 4(c), in which the characteristic peaks of MEN (22.6°) and the characteristic broad
276 diffraction peak of gelatin were observed respectively. It suggested that the gelatin
277 was modified with MEN after crosslinking reaction, which was consistent with the
278 FTIR results.

279 Fig. 2 here

280 3.2.3 Free -NH₂ in Gel-MEN film formation solution

281 Fig. 3 indicates the changing curve (a) of residual primary amino in Gel-MEN film
282 formation solution and gelatin liquid blending with ME (Gel/ME, curve b) against the
283 ratio δ ($\delta = m_{(MEN/ME)}/m_{(dry\ gelatin)}$). For Gel-MEN, the dosage of crosslinker played an
284 important role in the content of free -NH₂ while the free -NH₂ changed slightly no
285 matter how much ME was added. It suggested the stability of ester group in ME
286 which was not active enough to react with -NH₂ in gelatin. This meant that amine
287 groups in gelatin did not act as nucleophiles to break ester bonds in ME but could
288 break ester bonds in MEN. All these results confirmed the reaction process (scheme 1)
289 we proposed were correct. Interestingly, after activation by NHS, the active ester
290 MEN could consume -NH₂ in gelatin and dose dependent. The amount of free -NH₂
291 decreased sharply with the ratio δ increased from 0 to 25%, and then decreased
292 slightly when the ratio further increased. Specially, the amount of free -NH₂ reduced
293 down to a minimum value about 1.74×10^{-4} mol/g when $\delta = 30\%$. All these proved that
294 the whole system conquered the forbiddance of interfacial reaction. Compared with
295 former interface reaction study by Xu [47], in which gelatin was modified by glycidol
296 and the maximum -NH₂ conversion rate was 42%, the -NH₂ conversion rate in this
297 work was 28% higher than that reported.

298 Fig. 3 here

299 3.3 Performance of Gel-MEN films

300 3.3.1 Degradation properties in vitro

301 As sustained-release material, the composite films are expected to degrade with a
302 proper rate to match special needs and keep activity within service life. The
303 degradation behavior of films in a physiological environment plays an important role
304 in application as sustained-release material. The in vitro degradation performance of
305 Gel and Gel-MEN films in phosphate buffered saline (PBS, pH 7.40) at different
306 intervals was investigated. As shown in Fig. 4, the blank gelatin degraded rapidly
307 because of the large number of hydrophilic amino and carboxyl groups in gelatin
308 backbone. Besides, the physical structure of gelatin which possessed higher porosity
309 and leaner pore-wall contributed to the minimum weight remaining of 15% at 24 h.
310 The composite polymer Gel-MEN degraded proportionally slow because of the
311 incorporation of cellulosic crosslinker MEN. The weight remainings of Gel-25%MEN
312 and Gel-30%MEN at 24 h were 57% and 58% respectively, 40% greater than that of
313 original gelatin films. The amido bond formed between MEN and gelatin was stable
314 enough to resist adverse factor outside. It was reasonable to consider that strong
315 hydrogen bond and electrostatic interaction between gelatin polypeptide and
316 hydrophilic hydroxyl or carboxylic groups in MEN also depressed PBS medium
317 diffusion and protected gelatin polypeptide chains from degradation. Meanwhile, the
318 presence of MEN, a macromolecule crosslinker based on cellulose, also served as
319 physical crosslinking sites, which enhanced the stability of the network. To conclude,
320 MEN improved the anti-degradation performance of gelatin films and this guaranteed
321 its potential usage as sustained-released material in many fields, such as food
322 packages inside, medical engineering, controlled-release fertilizer in agriculture and
323 so on.

324 Fig. 4 here

325 3.3.2 Morphology evaluation

326 SEM photographs of blank films revealed a dense, smooth and compact structure
327 without any embossment or hole in Fig. 5 (a). The magnification times of first row (a_1 ,

328 b_1, c_1) was lower than that of second row (a_2, b_2, c_2). The introduction of cellulosic
329 crosslinker MEN destroyed the homogeneous film surface with slice-like or rod-like
330 macromolecule grafted on the covering of gelatin (Fig. 5 (b)). The inset of Fig. 5 (b₂)
331 clearly displayed the feature of MEN.

332 Besides, the SEM images provided very good evidence in favor of the in vitro
333 degradation of test sample (Gel-25%MEN). It can be seen from Fig. 5 (b) and (c) that
334 the film surface was almost plane and even, though combined with some sags and
335 crests before the degradation started. One hour after degradation, the porous structure
336 with irregularities and apertures can be observed on the surface of the composite film,
337 which confirmed that the internal structure of Gel-MEN polymeric film was started to
338 degrade in the liquid medium. It can be assumed that the degradation of films was
339 gradually penetrating deeper from the surface [48].

340 Fig. 5 here

341 3.3.3 Thermal stability

342 The thermal gravimetric analysis (TGA) and differential thermogravimetric curves
343 (DTG) of composite films are performed in Fig. 6 to investigate the thermal stability.
344 Curve a (Gel) and curve b (Gel/glycerol) were almost similar with two representative
345 peaks at 190.00-220.00 °C and 321.44 °C, which corresponded to the initial
346 decomposition temperature at 5% weight loss (T_i) and maximum weight loss
347 temperature (T_m) of gelatin. The special peak at 250.07 °C in curve b was due to the
348 blending of glycerol as plasticizer in blank gelatin film. The DTG patterns of
349 Gel-MEN presented three steps for weight loss at the temperatures around 100 °C,
350 250.07 °C and 320~350 °C, involving one strong and two weak endothermic peaks.
351 The first weight loss at the temperature around 100 °C and the second weight loss at
352 about 250.07 °C were similar to that of curve b. The third weight loss with a strong
353 endothermic peak at 320~350 °C was due to the incorporation of active ester MEN
354 into gelatin, and exhibited positive correlation with the dosage of crosslinker. This
355 demonstrated that the crosslinking effect of the cellulose-based crosslinker improved
356 thermal stability of the material to some degree as found in the literature. On the one
357 hand, the crosslinking reaction between gelatin and MEN with amido bonds formed

358 made the macromolecule structure more stable and impregnable. On the other hand,
359 the hydrogen bond and electrostatic interaction of special groups in gelatin and MEN
360 further strengthened the structure. All these provided effective reinforcement layer to
361 endure thermal degradation. As Fig. 6-1 and 6-2 shows, T_m reached maximum of
362 349.26 °C when δ ($\delta = m_{(MEN)}/m_{(dry\ gelatin)}$) was 25%.

363 The thermal properties of Gel-25%MEN and Gel/25%MCC in the presence of
364 glycerol were compared in Fig. 6-1 and 6-2, in which curve b consisted of four
365 decomposition stages. The four peaks at 104.42, 192.23, 250.72 and 359.12 °C were
366 resolved into four different components of water, gelatin, glycerol and MCC,
367 respectively. The obvious peak at 193.23 °C that almost disappeared in curve a
368 indicated the severe phase separation in Gel/MCC system. However, compared with
369 the typical T_m (309.10 °C) of MCC [49], the rising decomposition temperature of
370 359.12 °C in curve b may be caused by the hydrogen bond formed between gelatin and
371 MCC, which increased the thermal stability of Gel/MCC films.

372 Fig. 6 here

373 3.3.4 Mechanical properties

374 Mechanical properties, especially elasticity modulus (E_m) and elongation at break
375 (E_{ab}) are particularly crucial for sustained-materials used in many fields. Table 2
376 shows the thickness, tensile strength (T_s), E_m and E_{ab} of the Gel-MEN composite films.
377 The decreased T_s indicated that the modified films yielded lower stress than pure
378 gelatin film. The tensile strength increased with the crosslinker adding from
379 Gel-5%MEN to Gel-20%MEN, but decreased in Gel-25%MEN and Gel-30%MEN.
380 And these results were in accordance with the former work reported by Azeredo [50].
381 This may be caused by the fact that when the amount of the macromolecule crosslinker
382 was high, adding them to film may induce the development of a heterogeneous
383 structure with the presence of discontinuous areas, which produced lower tensile
384 strength. Similarly, Martucci [51] reported that the addition of dialdehyde starch in
385 gelatin resulted in lower T_s values than control film and explained this apparently
386 anomalous behavior. The fact that polymeric nature of dialdehyde starch did not
387 introduce severe restrictions within gelatin matrix as usually occurred with short chain

388 dialdehyde such as formaldehyde or glutaraldehyde, and some degree of phase
389 separation in gelatin- dialdehyde starch films could reduce the T_s , too. Fortunately, E_m
390 and E_{ab} tended to predict better elasticity and flexibility that indicating the new
391 material was not fragile any more. The E_{ab} of Gel-25%MEN was 31.96%, thirty times
392 of blank gelatin film while the E_m of Gel-25%MEN was 448.72 MPa, a quarter of
393 blank one, which was 1736.11 MPa. The reason was that the active ester group in
394 MEN could form covalent bonds with amino in gelatin polypeptide, and the
395 hydrophilic groups could form hydrogen bonds. And all the newly formed bonds
396 weakened the protein-protein interactions which was effective to stabilize the gelatin
397 network. Besides, MCC, the base of the crosslinker MEN, demonstrated to be an
398 effective nano-reinforcement for biopolymer films that can drastically influence the
399 mechanical properties of biomaterials [50]. All these contributed to better flexibility
400 of the new biologic polymer matrix.

401 Table 2 here

402 3.3.5 Hydrophobicity analysis by contact angles

403 Gelatin was a kind of hydrophilia material because of the functional groups: amino,
404 carboxyl, hydroxyl and so on. The water-sensitive property limited its application in
405 many fields and the hydrophobization was needed. Ninan [21] reported a new material
406 of gelatin/zeolite porous scaffold and the contact angle was found to increase from
407 88.6 °C to 108.0 °C with the increasing concentration of zeolites in gelatin. The
408 hydrophobic effect of the crosslinker MEN on gelatin was confirmed by the results of
409 water contact angle measurements (Fig. S5). The pure gelatin film (Fig. S5, a) with a
410 typical contact angle of 77.8° was because of the hydrophilic groups exposed in
411 gelatin chains. After crosslinked by MEN, the Gel-MEN films (Fig. S5, b and c)
412 presented a sharp increase to 125.1° and 135.5°, respectively. This was due to the
413 replacement of some surface amino groups in gelatin polypeptide with active ester
414 groups in MEN. Besides, the hydrogen bonds formed between hydrophilic groups of
415 gelatin backbone and MCC-based crosslinker also contributed to good hydrophobicity
416 of modified gelatin films. The modified films with perfect hydrophobicity overcame
417 the permanent weakness of water-sensitive in the application of gelatin. And the

418 advanced properties broadened its usage as more kinds of material.

419 3.3.6 Water uptake studies

420 The hydrophilic property of gelatin can be controlled in two ways. One was
421 hydrophobization referred above, and the other was expected to absorb water
422 molecules. This happened because of two beneficial structure features of gelatin. One
423 advantage of gelatin materials was its highly hygroscopic nature due to which it
424 swelled and transformed to any shape easily in humid environment. The other was the
425 porosity in the network that allowed more water to enter inside, because which the
426 porous gelatin films showed higher swelling capacity. Water uptake (%) of pure
427 gelatin films and Gel-MEN composites tested during 11 days are shown in Fig. 7. The
428 water uptake (%) can be controlled by incorporating different dosages of MEN in the
429 polymer matrix. In the case of Gel-15%MEN, the water uptake (%) reached the
430 maximum among all MEN crosslinked gelatin films. This was attributed to the
431 increase in pore size of gelatin film with the presence of MEN. Additionally, the
432 Gel-MEN composites showed an increase in the swelling capacity till the 11th day,
433 which indicated a better ability of water absorbing. By comparison, the original
434 gelatin film acquired maximum swelling capacity on the 10th day and thereafter
435 percentage of water uptake was found to be invariant even decline. This event
436 suggested that introduction of MEN into gelatin provided effective channel for water
437 molecules to diffuse into the polymer matrix, thereby swelling ability increased.
438 Uncontrolled swelling properties can badly affect the mechanical property, so it was
439 advantageous to tune the swelling capacity [52].

440 Fig. 7 here

441 3.3.7 Light resistance performance

442 Many researches indicated that ultraviolet radiation was one of the main reason
443 causing skin hurting, light aging and skin cancer. Hence the low light transmission
444 also made the active gelatin film possess some health function [24]. Light
445 transmission at the selected wavelengths from 200 to 800 nm in UV and visible
446 ranges and transparency values of gelatin films are shown in Table 3 (& Fig. S6).
447 Comparison of the results with control films revealed that lower light transmittance (T)

448 was found in Gel-MEN composite films. And the films with 30%MEN displayed the
449 lowest values among them. This revealed that the addition of MEN improved the UV
450 barrier properties of gelatin films, resulting from the amido bonds by Schiff base
451 formation between the active ester groups in MEN and the amino groups of lysine or
452 hydroxylysine side groups in gelatin. Based on transparency values (T_v , Table 3), the
453 more crosslinker led to the greater T_v , which represented the opacity of resulted films.
454 The opacity was highly influenced by the crystalline content of a sample: more
455 compact polymer chains made it more difficult for light passing through and then the
456 opacity of films was increased [53]. All these indicated that protein-based films were
457 considered to exhibit high UV barrier properties, owing to their high content of
458 aromatic amino acids which absorbed UV light.

459 Table 3 also displays the light barrier properties of Gel/15%MCC and
460 Gel/25%MCC blending films, as compared with the corresponding mass ratio of
461 Gel-MEN films. The Gel/MCC blending films exhibited better transparency while
462 worse light resistance performance. This fact may be an indication that MCC
463 nanoparticles were homogeneously distributed in the matrix because they are white,
464 and light incident on the film surface was reflected in larger quantity due to the white
465 particles [25]. The light barrier properties of films were relatively important while
466 used as sustained-materials for food packaging or food coating. The polymer matrix in
467 this work just matched these needs.

468 Table 3 here

469 4. Conclusion

470 In summary, the structure and conformation of gelatin were modified by the
471 macromolecule crosslinker MEN. The FTIR spectra, elemental analysis and TGA
472 values verified the structure of MEN. Reaction between $-NH_2$ in gelatin and active
473 ester in MEN was confirmed by residual primary amino test, FTIR and XRD spectra,
474 which broke the limitation of blending modification method for gelatin with
475 macromolecule. Dose-dependent effect of crosslinker was investigated through
476 degradation in vitro, in which the weight remaining decreased with the increase of
477 MEN dosage. The SEM images further proved the successful surface grafting reaction
478 and the degradation phenomenon in PBS medium. The decomposition temperature

479 obtained from TGA curves increased to 350 °C compared with the native film of 320
480 °C. Besides, TGA patterns of Gel-MCC composites exhibited serious phase separation.
481 The mechanical properties changed to some degree with higher E_{ab} and lower E_m ,
482 which suggested better flexible and shatter-proof. The contact angles with high value
483 of 135.5° indicated good hydrophobic properties. The swelling ability after absorbing
484 water could be regulated by adding different weight of crosslinker. The light barrier
485 performance was improved since the introduction of MEN compared with both pure
486 gelatin film and Gel/MCC composites. Giving the application status of gelatin, our
487 study is the extension of existing NHS crosslinking technique and will broaden the
488 application of gelatin films as sustained-released material in food industry, medicine,
489 agriculture and so on .

490 **Acknowledgment**

491 We gratefully acknowledge the promotive research fund for young and middle-aged
492 scientists of Shandong Province (BS2014NJ012), the National Natural Science
493 Foundation of China (NO.21276149) and the Program for Scientific Research
494 Innovation Team in Colleges and Universities of Shandong Province.

495 **References**

- 496 [1] L. B. Guan, W. H. Dan et al. Gelatin and its Application in Biomedical Material [J]. Material
497 Reviews, 2006, 20: 380-383.
- 498 [2] D. Narayanan, Geena M. G, Lakshmi H, M. Koyakutty, S. Nair, D. Menon. Poly-(ethylene
499 glycol) modified gelatin nanoparticles for sustained delivery of the anti-inflammatory drug
500 Ibuprofen-Sodium: An in vitro and in vivo analysis [J]. Nanomedicine: Nanotechnology,
501 Biology, and Medicine, 2013, 9: 818-828.
- 502 [3] Yang Lu. The research progress of gelatin microspheres [J]. The science and Technology of
503 Gelatin, 2006, 26(2): 57-70.
- 504 [4] Yang Lu. The study development of gelatin microballoon sphere [J]. The science and
505 Technology of Gelatin, 2006, 26(3): 113-134.
- 506 [5] Ajit P. Rokhade, Sunil A. Agnihotri, Sangamesh A. Patil, Nadagouda N. Mallikarjuna,
507 Padmakar V. Kulkarni, Tejraj M. Aminabhavi. Semi-interpenetrating polymer network
508 microspheres of gelatin and sodium carboxymethyl cellulose for controlled release of ketorolac
509 tromethamine [J]. Carbohydrate Polymers, 2011, 65: 243-252.
- 510 [6] Bhavesh D. Kevadiya, Shalini Rajkumar, Hari C. Bajaj, Shiva Shankaran Chettiar, Kalpeshgiri
511 Gosai, Harshad Brahmhatt, Adarsh S. Bhatt, Yogesh K. Barvaliya, Gaurav S. Dave, Ramesh
512 K. Kothari. Biodegradable gelatin-ciprofloxacin-montmorillonite composite hydrogels for
513 controlled drug release and wound dressing application [J]. Colloids and Surfaces B:
514 Biointerfaces, 2014, 122: 175-183.
- 515 [7] P. V. Kozlov, G. I. Burdygina. The structure and properties of solid gelatin and the principles of
516 their modification [J]. Polymer Reviews, 1983, (24): 651-666.
- 517 [8] Yongmei Cao, Kelin Huang, Rui Wu, Ben Wang, Hongyu Liu, Shangshun Huang, Yaoliang
518 He, Weiguo Li. Characteristics, Applications and Market Prospect of Microcrystalline
519 Cellulose [J]. Enterprise Science And Technology & Development, 2009, (12), 48-51.
- 520 [9] Ana Casas, Salama Omar, Jose Palomar, Mercedes Oliet, M. Virginia Alonso, Francisco
521 Rodriguez. Relation between differential solubility of cellulose and lignin in ionic liquids and
522 activity coefficients [J]. RSC Adv., 2013, 3: 3453-3460.
- 523 [10] Yuehan Wu, Xingzhong Zhang, Bin Lia, Shilin Liu. Highly transparent and flexible
524 silica/cellulose films with a low coefficient of thermal expansion [J]. RSC Adv., 2014, 4:

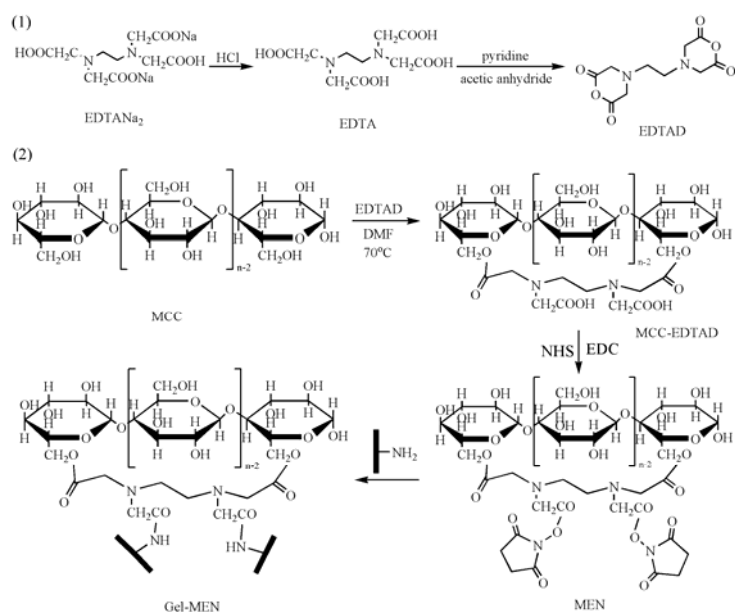
- 525 52349-52356.
- 526 [11] Oihana Gordobil, Itziar Egüés, Inaki Urruzola, Jalel Labidi. Xylan-cellulose films:
527 Improvement of hydrophobicity, thermal and mechanical properties Oihana [J]. Carbohydrate
528 Polymers, 2014, 112: 56-62.
- 529 [12] Yasemin Numanoğlu, Sibel Sungur. β -Galactosidase from *Kluyveromyces lactis* cell
530 disruption and enzyme immobilization using a cellulose-gelatin carrier system [J]. Process
531 Biochemistry, 2004, 39: 703-709.
- 532 [13] Shih-Ta Chang, Li-Chen Chen, Shih-Bin Lin, Hui-Huang Chen. Nano-biomaterials
533 application: Morphology and physical properties of bacterial cellulose/gelatin composites via
534 crosslinking [J]. Food Hydrocolloids, 2012, 27: 137-144.
- 535 [14] Shengying Qin. EDTA Dianhydride and Their Derivatives [J]. Chemical Research and
536 Application, 1993, 5(4): 1-13.
- 537 [15] Yun Xing, Dong Liu, Li-Ping Zhang. Enhanced adsorption of Methylene Blue by
538 EDTAD-modified sugarcane bagasse and photocatalytic regeneration of the adsorbent [J].
539 Desalination, 2010, 259: 187-191.
- 540 [16] Yanfeng Luo, Hui Peng, Jinchuan Wu, Jiaoxia Sun, Yuanliang Wang. Novel amphoteric
541 pH-sensitive hydrogels derived from ethylenediaminetetraacetic dianhydride, butanediamine
542 and amino-terminated poly(ethylene glycol): Design, synthesis and swelling behavior [J].
543 European Polymer Journal, 2011, 47: 40-47.
- 544 [17] Chao Yang, Ling Xua, Ying Zhou, Xiangmei Zhang, Xin Huang, Min Wang, Ye Han, Maolin
545 Zhai, Shicheng Wei, Jiuqiang Li. A green fabrication approach of gelatin/CM-chitosan
546 hybrid hydrogel for wound healing [J]. Carbohydrate Polymers, 2010, 82: 1297-1305.
- 547 [18] C. Abrusci, D. Marquina, A. Del Amo, F. Catalina. Biodegradation of cinematographic
548 gelatin emulsion by bacteria and filamentous fungi using indirect impedance technique [J].
549 International Biodeterioration & Biodegradation, 2007, 60: 137-143.
- 550 [19] J.F. Martucci, R.A. Ruseckaite. Biodegradation of three-layer laminate films based on gelatin
551 under indoor soil conditions [J]. Polymer Degradation and Stability, 2009, 94: 1307-1313.
- 552 [20] S. Lotfy, Y. H. A. Fawzy. Characterization and enhancement of the electrical performance of
553 radiation modified poly (vinyl) alcohol/gelatin copolymer films doped with carotene [J].
554 Journal of Radiation Research and Applied Sciences, 2014, 7: 338-345.

- 555 [21] Neethu Ninan, Yves Grohens, Anne Elain, Nandakumar Kalarikkal, Sabu Thomas. Synthesis
556 and characterisation of gelatin/zeolite porous scaffold [J]. *European Polymer Journal*, 2013,
557 49: 2433-2445.
- 558 [22] Emo Chiellinia, Patrizia Cinelli, Andrea Corti, El Refaye Kenawy. Composite films based on
559 waste gelatin: thermal–mechanical properties and biodegradation testing [J]. *Polymer*
560 *Degradation and Stability*, 2001, 73, 549-555.
- 561 [23] Mourad Jridi, Sawssan Hajji, Hanen Ben Ayed, Imen Lassoued, Aïcha Mbarek, Maher
562 Kammoun, Nabil Souissi, Moncef Nasri. Physical, structural, antioxidant and antimicrobial
563 properties of gelatin-chitosan composite edible films [J]. *International Journal of Biological*
564 *Macromolecules*, 2014, 67: 373-379.
- 565 [24] Jian-Hua Li, Jing Miao, Jiu-Lin Wu, Shan-Fei Chen, Qi-Qing Zhang. Preparation and
566 characterization of active gelatin-based films incorporated with natural antioxidants [J]. *Food*
567 *Hydrocolloids*, 2014, 37: 166-173.
- 568 [25] J.S. Alves, K.C. dos Reis, E.G.T. Menezes, F.V. Pereira, J. Pereira. Effect of cellulose
569 nanocrystals and gelatin in corn starch plasticized films [J]. *Carbohydrate Polymers*, 2015,
570 115: 215-222.
- 571 [26] R. Andrade, O. Skurtys, F. Osorio, R. Zuluaga, P. Gañán, C. Castro. Wettability of gelatin
572 coating formulations containing cellulose nanofibers on banana and eggplant epicarps [J].
573 *LWT - Food Science and Technology*, 2014, 58: 158-165.
- 574 [27] Yongmei Cheng, Jinting Lua, Shilin Liu, Peng Zhao, Guozhong Lu, Jinghua Chen. The
575 preparation, characterization and evaluation of regenerated cellulose/collagen composite
576 hydrogel films [J]. *Carbohydrate Polymers*, 2014, 107: 57-64.
- 577 [28] Changdao Mu, Jimin Guo, Xinying Li, Wei Lin, Defu Li. Preparation and properties of
578 dialdehyde carboxymethyl cellulose crosslinked gelatin edible films [J]. *Food Hydrocolloids*,
579 2012, 27: 22-29.
- 580 [29] M. Zhang, K. Wu, G. Y. Li. Interactions of collagen molecules in the presence of
581 N-hydroxysuccinimide activated adipic acid (NHS-AA) as a crosslinking agent [J].
582 *International Journal of Biological Macromolecules*, 2011, 49: 847-854.
- 583 [30] T. Kajiyama, H. Kobayashi, T. Taguchi, H. Saito, Y. Kamatsua, K. Kataoka, J. Tanaka.
584 Synthesis of activated poly (α,β -malic acid) using N-hydroxysuccinimide and its gelation

- 585 with collagen as biomaterials [J]. *Materials Science and Engineering: C*, 2004, 24: 815-819.
- 586 [31] H. Saito, T. Taguchi, H. Aoki, S. Murabayashi, Y. Mitamura, J. Tanaka, T. Tateishi.
587 PH-responsive swelling behavior of collagen gels prepared by novel crosslinkers based on
588 naturally derived di- or tricarboxylic acids [J]. *Acta Biomater*, 2007, (3): 89-94.
- 589 [32] Osvaldo Karnitz Júnior, Leandro Vinícius Alves Gurgel, Rossimiriam Pereira de Freitas,
590 Laurent Frédéric Gil. Adsorption of Cu(II), Cd(II), and Pb(II) from aqueous single metal
591 solutions by mercerized cellulose and mercerized sugarcane bagasse chemically modified
592 with EDTA dianhydride (EDTAD) [J]. *Carbohydrate Polymers*, 2009, 77: 643-650.
- 593 [33] Osvaldo Karnitz Jr., Leandro Vinicius Alves Gurgel, Ju' lio Ce'sar Perin de Melo, Vagner
594 Roberto Botaro, Ta'nia Ma'rcia Sacramento Melo, Rossimiriam Pereira de Freitas Gil,
595 Laurent Fre'de'ric Gil. Adsorption of heavy metal ion from aqueous single metal solution by
596 chemically modified sugarcane bagasse [J]. *Bioresource Technology*, 2007, 98: 1291-1297.
- 597 [34] Karla Aparecida Guimarães Gusmão, Leandro Vinícius Alves Gurgel, Tânia Márcia
598 Sacramento Melo, Laurent Frédéric Gil. Adsorption studies of methylene blue and gentian
599 violet on sugarcane bagasse modified with EDTA dianhydride (EDTAD) in aqueous
600 solutions: Kinetic and equilibrium aspects [J]. *Journal of Environmental Management*, 2013,
601 118: 135-143.
- 602 [35] Osvaldo Karnitz Júnior, Leandro Vinícius Alves Gurgel, Laurent Frédéric Gil. Removal of
603 Ca(II) and Mg(II) from aqueous single metal solutions by mercerized cellulose and
604 mercerized sugarcane bagasse grafted with EDTA dianhydride (EDTAD) [J]. *Carbohydrate*
605 *Polymers*, 2010, 79: 184-191.
- 606 [36] Y. H. Chen, M. Zhang, W. T. Liu, G. Y. Li. Properties of alkali-solubilized collagen solution
607 crosslinked by N-hydroxysuccinimide activated adipic acid [J]. *Korea-Australia Rheology*
608 *Journal*, 2011, 23: 41-48.
- 609 [37] D. D. Van Slyke. A method for quantitative determination of aliphatic amino groups:
610 applications to the study of proteolysis and proteolytic products [J]. *Biol. Chem*, 1911, (9):
611 185-204.
- 612 [38] L. D. Li. Quantometer of amino [P]. China. 201220241965.6. 2012-05-28.
- 613 [39] A. A. Haroun, E. F. Ahmed, M. A. Abd El-Ghaffar. Preparation and antimicrobial activity of
614 poly(vinylchloride)/gelatin/montmorillonite biocomposite films [J]. *J Mater Sci: Mater Med*,

- 615 2011, (22): 2545-2553.
- 616 [40] Phakawat Tongnuanchan, Soottawat Benjakul, Thummanoon Prodpran. Properties and
617 antioxidant activity of fish skin gelatin film incorporated with citrus essential oils [J]. Food
618 Chemistry, 2012, 134(3): 1571-1579.
- 619 [41] Y. FANG, M. A. TUNG, I. J. BRITT, S. YADA, D. G. DALGLEISH. Tensile and Barrier
620 Properties of Edible Films Made from Whey Proteins [J]. Journal of food science, 2002, 67:
621 188-193.
- 622 [42] Gholamreza Kavooosi, Aytak Rahmatollahi, Seyed Mohammad Mahdi Dadfar, Amin
623 Mohammadi Purfard. Effects of essential oil on the water binding capacity,
624 physicochemical properties, antioxidant and antibacterial activity of gelatin films [J].
625 LWT-Food Science and Technology, 2014, 57: 556-561.
- 626 [43] Xuejing Zheng, Jie Liu, Ying Pei, Junwei Li, Keyong Tang. Preparation and properties of
627 sisal microfibril/gelatin biomass composites [J]. Composites: Part A, 2012, 43: 45-52.
- 628 [44] KUNIHICO WATANABE, MARI TABUCHI, YASUSHI MORINAGA AND FUMIHIRO
629 YOSHINAGA. Structural features and properties of bacterial cellulose produced in agitated
630 culture [J]. CELLULOSE, 1998, 5: 187-200.
- 631 [45] Chang Seok Ki, Doo Hyun Baek, Kyung Don Gang, Ki Hoon Lee, In Chul Um, Young Hwan
632 Park. Characterization of gelatin nanofiber prepared from gelatin–formic acid solution [J].
633 Polymer, 2005, 46: 5094-5102.
- 634 [46] J. Wang, Y. Z. Wan, H. L. Luo, C. Gao, Y. Huang. Immobilization of gelatin on bacterial
635 cellulose nanofibers surface via crosslinking technique [J]. Materials Science and
636 Engineering C, 2012, 32: 536-541.
- 637 [47] J. Xu, T. D. Li, X. L. Tang, C. D, Qiao, Q, W, Jiang. Effect of aggregation behavior of gelatin
638 in aqueous solution on the grafting density of gelatin modified with glycidol [J]. Colloids and
639 Surfaces B: Biointerfaces, 2012, (95): 201-207.
- 640 [48] Niladri Roy, Nabanita Saha, Takeshi Kitano, Petr Saha. Biodegradation of PVP-CMC
641 hydrogel film: A useful food packaging material [J]. Carbohydrate Polymers, 2012, 89:
642 346-353.
- 643 [49] Dekui Shen, Rui Xiao, Sai Gu, Kaihong Luo. The pyrolytic behavior of cellulose in
644 lignocellulosic biomass: a review [J]. RSC Adv., 2011, 1: 1641-1660.

- 645 [50] Talita M. Santos, Men de Sá M. Souza Filho, Carlos Alberto Caceres, Morsyleide F. Rosa,
646 João Paulo S. Morais, Alaídes M.B. Pinto, Henriette M.C. Azeredo. Fish gelatin films as
647 affected by cellulose whiskers and sonication [J]. Food Hydrocolloids, 2014, 41: 113-118.
- 648 [51] Martucci J F, Ruseckaite R A. Tensile properties, barrier properties, and biodegradation in
649 soil of compression-molded gelatin-dialdehyde starch films. [J]. Journal of Applied Polymer
650 Science, 2009, 112: 2166-2178.
- 651 [52] A. Bigi, G. Cojazzi, S. Panzavolta, K. Rubini, N. Roveri. Mechanical and thermal properties
652 of gelatin films at different degrees of glutaraldehyde crosslinking [J]. Biomaterials, 2001, 22:
653 763-768.
- 654 [53] Matsuguma L. S., Lacerda L. G., Schnitzler E., Carvalho Filho M. A. d., Franco S., Demiate
655 C. M. L. I. M. Characterization of native and oxidized starches of two varieties of Peruvian
656 carrot (*Arracacia xanthorrhiza*, B.) from two production areas of Paraná state, Brazil.
657 Brazilian Archives of Biology and Technology, 2009, 52, 701-713.
658



659

660

661

Scheme 1 The formation process of crosslinked gelatin with MEN.

(1). The synthetic route of EDTA anhydride (EDTAD);

662

663

(2). The preparation path of gelatin modified with MEN.

664

665 **Figure and Table captions:**

666 **Fig. 1** The FTIR spectra of MEN, gelatin and Gel-MEN

667 **Fig. 2** The XRD patterns of MEN, gelatin and Gel-MEN

668 **Fig. 3** Residual amino group content of gelatin solution modified by MEN (a) and ME (b) with
669 different dosages

670 **Fig. 4** Effect of macromolecule crosslinker on in vitro degradation of the Gel-MEN composite
671 films

672 **Fig. 5** Film Surface morphology of Gel (a₁, a₂), Gel-25%MEN (b₁, b₂) and Gel-25%MEN after 1 h
673 degradation (c₁, c₂)

674 **Fig. 6** TGA and DTG curves of modified gelatin films with different dosage of crosslinker (6-1,
675 6-2) and comparison curves between Gel-25%MEN and Gel/25%MCC blending films (6-3, 6-4)

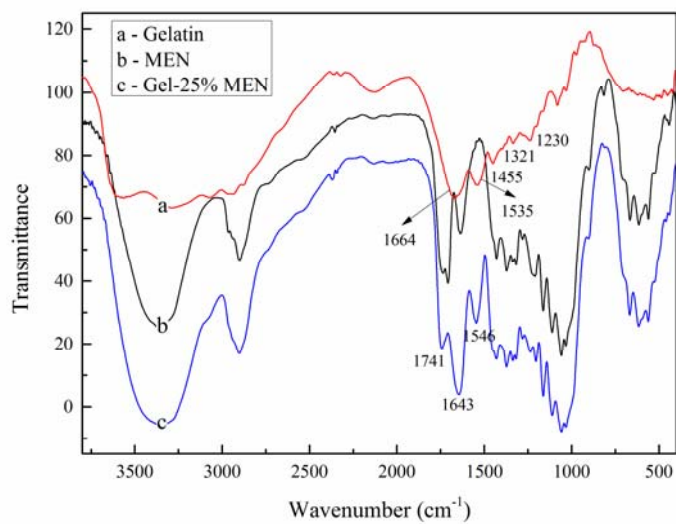
676 **Fig. 7** Water uptake properties of gelatin films incorporated with different dosage of MEN

677

678 **Table 1** Elemental analysis and thermal property values of MCC, ME and MEN

679 **Table 2** Mechanical performance of different Gel-MEN films

680 **Table 3** Light transmission and transparency values of different Gel-MEN films

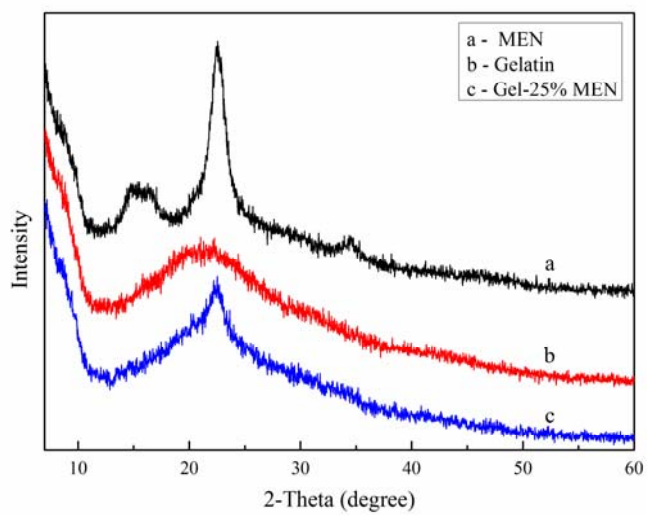


681

682

683

Figure 1

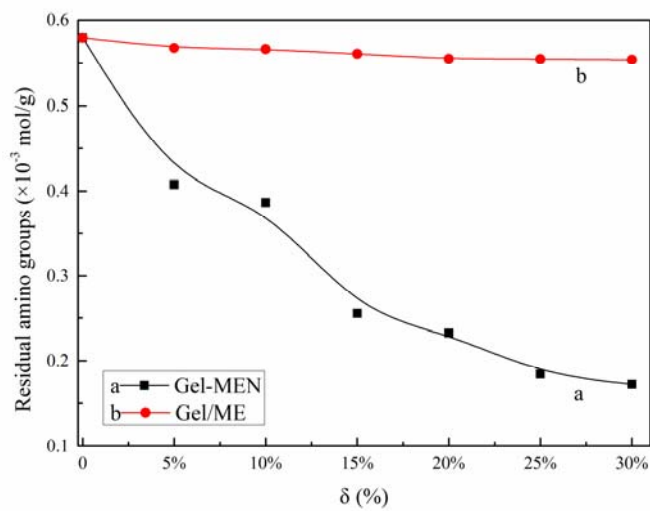


684

685

686

Figure 2

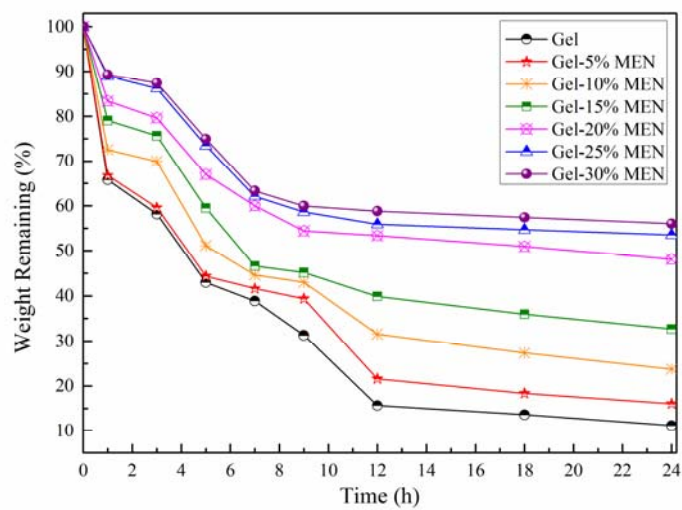


687

688

689

Figure 3

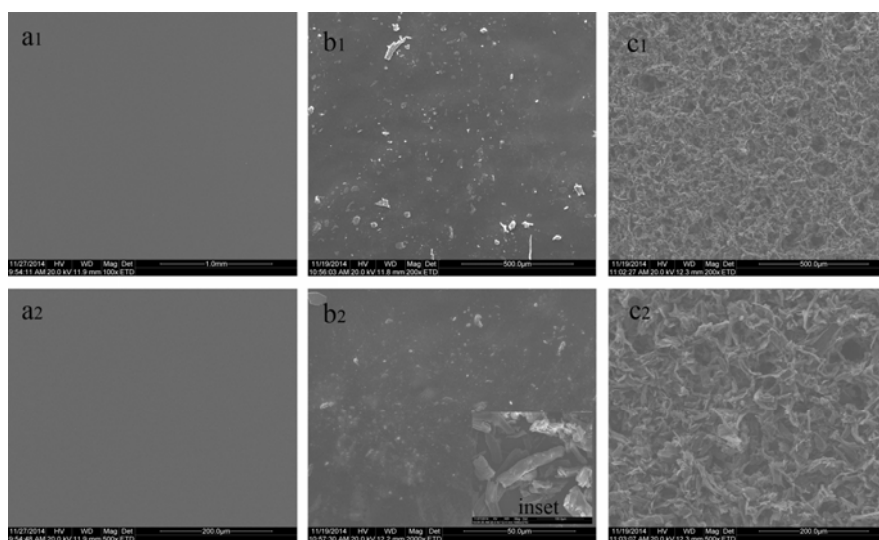


690

691

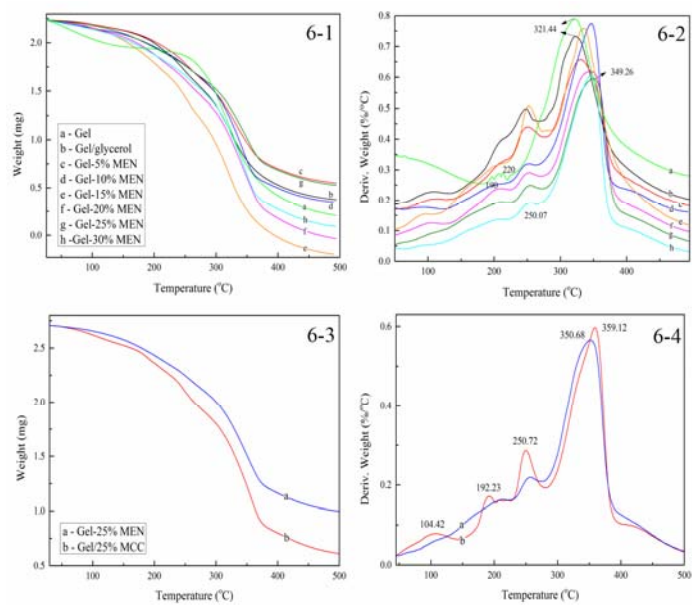
692

Figure 4



693
694
695

Figure 5

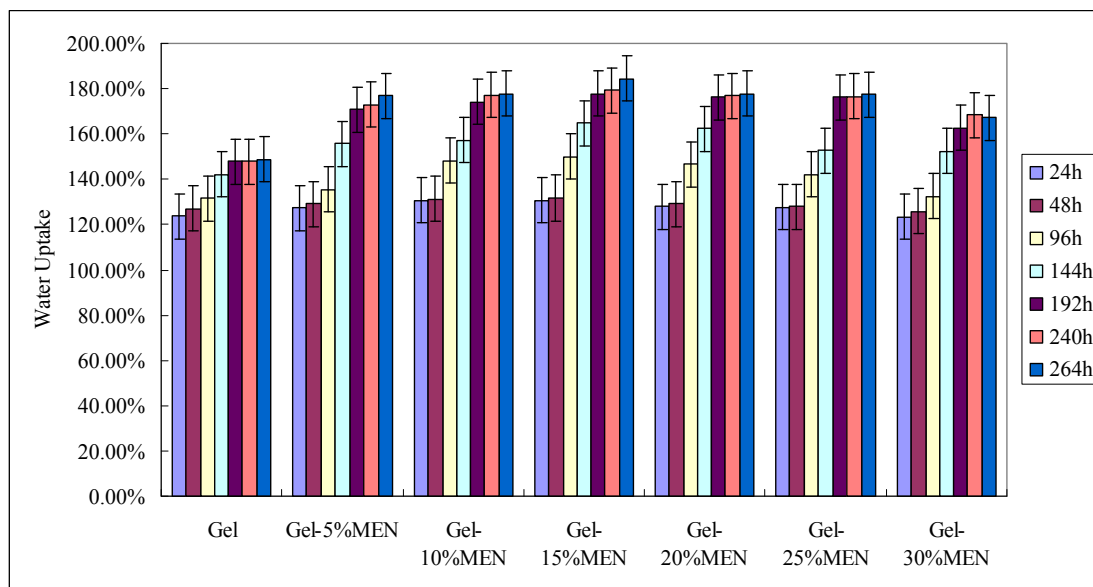


696

697

698

Figure 6



699

700

701

Figure 7

702

Table 1

Materials	C (%)	H (%)	N (%)	Weight gain (%)	T _i (°C)	T _m (°C)	T _g (°C)	Residue (%)
MCC	42.21	6.40	0.11	-	309.10	364.08	340.68	15.28
ME	42.29	6.45	1.92	72.50	271.45	331.50	342.70	33.01
MEN	42.97	6.65	2.48	30.80	222.54	377.31	364.09	10.45

703

Table 2

Films	Thickness (mm)	Tense Strength (MPa)	Elongation at Break (%)	Elasticity Modulus (MPa)
Gel	0.10	24.17	1.84	1736.11
Gel-5%MEN	0.18	15.28	7.64	435.73
Gel-10%MEN	0.20	16.17	11.52	468.75
Gel-15%MEN	0.20	18.25	12.44	595.24
Gel-20%MEN	0.28	18.10	28.64	525.21
Gel-25%MEN	0.26	13.97	31.96	448.72
Gel-30%MEN	0.20	14.08	83.08	476.19

704

Table 3

Films	Wavelength (nm)										Transparency Value	
	200	280	350	400	450	500	550	600	700	800	280	600
Gel	2.2	1.5	43.2	55.0	59.7	62.6	64.4	66.5	67.6	68.5	10.13	0.98
Gel-MEN5%	1.5	5.8	29.8	34.4	35.4	36.4	37.0	37.8	38.4	39.0	7.73	2.64
Gel-MEN10%	0.6	2.6	12.4	14.4	15.1	15.5	15.8	16.2	16.4	16.4	11.32	5.65
Gel-MEN15%	0.2	0.2	4.4	5.8	6.3	6.6	6.7	7.1	7.1	7.2	13.49	5.74
Gel-MEN20%	0.1	0.2	2.2	3.0	3.5	3.6	3.7	3.7	3.7	3.7	13.49	7.16
Gel-MEN25%	0	0	0.6	1.0	1.3	1.4	1.5	1.6	1.6	1.6	---	8.98
Gel-MEN30%	0	0	0.4	0.6	0.9	1.0	1.1	1.1	1.1	1.1	---	9.79
Gel/MCC15%	1.9	9.3	34.6	39.6	40.9	42.3	43.3	45.1	46.5	47.7	10.32	3.46
Gel/MCC25%	1.4	5.3	26.6	31.7	33.0	34.4	35.5	36.9	38.0	39.3	12.78	4.32

705

706